7.1 RELATIONSHIP BETWEEN EULERIAN AND LAGRANGIAN STATISTICS IN THE STUDY OF ATMOSPHERIC DISPERSION IN THE CONVECTIVE BOUNDARY LAYER: A LARGE-EDDY SIMULATION STUDY

Alessandro Dosio *, **Jordi Vilà-Guerau de Arellano, Albert A.M. Holtslag,**
Meteorology and Air Quality Group, Wageningen University, Wageningen, The Netherlands
Peter J.H. Builtjes
TNO-MEP, Apeldoorn, The Netherlands

1. INTRODUCTION

Atmospheric dispersion is a topic of great importance especially in relation to pollutant transport. Two different approaches, known as the *Eulerian* and the *Lagrangian* frameworks, are used to describe this process.
In the Eulerian framework, statistical properties are calculated in a fixed reference frame. This approach is most commonly used in field experiments as well as in laboratory experiments or Eulerian numerical models.
In the Lagrangian framework the statistical properties are calculated in a reference frame which moves with the flow. This is the most natural approach for theoretical investigation of turbulent dispersion, as in the works by Taylor (1921) who established seminal theoretical relationships between dispersion parameters and turbulent characteristics.
Experimental measures of Lagrangian statistics in the atmospheric Convective Boundary Layer (CBL) are very difficult to obtain, (Hanna, 1981), whereas experiment with grid-generated isotropic turbulence (e.g. Sato and Yamamoto, 1987) are only partially representative of the turbulent motion in the CBL.
A suitable approach for studying Lagrangian statistics in the CBL is by Large Eddy Simulation (LES), i.e. trajectories of particles released in a numerically generated turbulent flow are tracked in space and time.
In this study we used a LES to address three main research issues:
First, the turbulent characteristics of the flow are studied in both Eulerian and Lagrangian frameworks by analyzing velocity autocorrelations and calculating integral scales.
Second, the relationship between flow properties (autocorrelations) and dispersion characteristics (particles' displacements) is discussed through Taylor's analysis of turbulent dispersion (Taylor, 1921). The influence of the asymmetry of the CBL flow on dispersion is studied, with the focus being on the difference between horizontal and vertical motion.
Finally, the relationship between Eulerian and Lagrangian frameworks is studied by calculating the ratio β between the Lagrangian and Eulerian time scales.

* *Corresponding author address:* A. Dosio, Wageningen University, Meteorology and Air quality Group, 6701 AP Wageningen, The Netherlands; e-mail: alessandro.dosio@wur.nl

2. THEORETICAL BACKGROUND

Dispersion in the atmosphere is related to the displacement of particles from one other. Assuming an ensemble of particles moving in the turbulent flow, the displacement in the j^{th} direction, at a time t after the release, is defined as:

$$\overline{x_j'^2}(t) = \overline{\left(x_j^i(t) - \overline{x_j^i(t)}\right)^2} \tag{1}$$

where $x_j^i(t)$ is the position of the i^{th} particle and the overbar represents the average over all the particles.
Following the classical analysis of Taylor (1921), this displacement is expressed as a function of the properties of the turbulent flow according to:

$$\overline{x_j'^2}(t) = 2\sigma_j^2 \int_0^t \int_0^{t'} R_j^L(\tau) d\tau dt' \tag{2}$$

where σ_j is the (square root of the) velocity variance, and $R_j^L(\tau)$ is the Lagrangian autocorrelation function, defined as:

$$R_j^L(\tau) = \frac{\overline{u_j'(t) u_j'(t+\tau)}}{\sigma_j^2}. \tag{3}$$

Here, $u_j'(t) = u_j^i(t) - \overline{u_j^i(t)}$ is the velocity fluctuation of the i^{th} particle at time t and τ is the time lag.
Relationship (2) has two analytical limits for short and large times, respectively:

$$\overline{x_j'^2}(t) = \sigma_j^2 t^2 \qquad t << T_j^L \tag{4}$$

$$\overline{x_j'^2}(t) = 2\sigma_j^2 T_j^L t \qquad t >> T_j^L \tag{5}$$

where the *Lagrangian (integral) time scale* T_j^L is defined as:

$$T_j^L \equiv \int_0^\infty R_j^L(\tau) d\tau \tag{6}$$

Lagrangian statistics are seldom measured experimentally in the CBL and T_j^L is normally inferred from Eulerian statistics using the following relationship:

$$T_j^L = \beta_j T_j^E \tag{7}$$

where T_j^E is the Eulerian integral time scale and β_j is the ratio of the Lagrangian to Eulerian timescales.

3. NUMERICAL SETUP

The LES code used here is the parallelized version of the one described by Siebesma and Cuijpers(1995), in which a set of filtered prognostic equations for the dynamic variables (wind velocity, potential temperature, turbulent kinetic energy) is solved on a staggered numerical grid. The subgrid fluxes are closed by relating them to the gradient of the solved variable by means of an exchange coefficient which depends on the subgrid turbulent kinetic energy and a length scale. The space and time integrations are computed with a Kappa (Vreugdenhil and Koren, 1993) and leap-frog numerical schemes respectively. The numerical domain covers an area of 10.240 x 10.240 km^2. A horizontal grid length of 40 m is used (256 grid points in each horizontal direction). A non uniform grid of 96 points was used in the vertical direction, with the vertical grid resolution varying from 5 m near to the surface to 15 m above the surface layer. The aspect ratio, i.e. the ratio between the horizontal domain dimension to the CBL height z_i, is around 10. Lateral periodic boundary conditions are imposed for all the variables. A time step of 0.25 s. is used. A geostrophic wind of $5m/s$ aligned in the x-direction and a heat flux of 0.156 $K.m/s$ are imposed as constant forcing. At the top of the CBL, a inversion strength of $\Delta\theta = 5K$ was imposed, which strongly limits the vertical motion of the flow in the entrainment zone. The flow is characterized by the shear/buoyancy ratio $u*/w*$ equal to 0.21 (where u_* is the friction velocity and w_* the convective velocity scale). The value of the stability parameter $-z_i/L$ is ~ 40. According to the classification used in Holtslag and Nieuwstadt (1986) this simulated flow is mainly driven by convective turbulence.

3.1 *Lagrangian particle model*

After an initialization period of 2 hours (i.e. the period of CBL development needed to ensure that a (quasi-) stationary state is reached), 1024 particles were released on a regular horizontal grid at 50 different levels (from $z = 100\ m$ to $z = 850\ m$) i.e. a total of 51200 particles. The position and velocity of each particle was recorded every 5 seconds for the following 5120 s.
The position in direction j of the i^{th} particle was calculated according to:

$$x_j^i(t + \Delta t) = x_j^i(t) + u_j^i(t)\Delta t \qquad (8)$$

where Δt is the time step and $u_j^i(t)$ is the velocity of the particle calculated by interpolating linearly the values of the resolved (Eulerian) velocity at the eight closest grid points. As pointed out by Weil et al. (2004), a more realistic calculation of the particles' position should include in (8) the subgrid component of the velocity $u_j^{i'}$, which is not directly available from the LES. It is important to notice that the Lagrangian statistics (both autocorrelations and integral scales) are associated with the largest scale of motion, which are explicitly solved by the LES and therefore the velocity subgrid scales are not very relevant. This is corroborated by previous studies by Wang et al. (1995) and by Gopalakrishnan and Avissar (2000) (personal communication) who found no significative difference in the results if the velocity subgrid component was taken into account. The subgrid velocity $u_j^{i'}$ was therefore not included in our calculations

4. EULERIAN STATISTICS

Eulerian statistics are calculated in a fixed framework. Eulerian length and time scales have already been investigated in a large number of studies, both experimentally and numerically. However, there is an essential difference between field experiments and numerical studies. Field experiments (e.g Hanna, 1981) usually provide temporal statistics (i.e. statistics derived by the analysis of time series collected in fixed positions), whereas in numerical (e.g Mason, 1989) or laboratory experiments (e.g Deardorff and Willis, 1985) data are collected at different locations at a fixed time (or averaged over a certain time). These two analysis are usually related by Taylor's hypothesis of frozen turbulence, which is always assumed but seldom validated. Here we analyze both time and spatial statistics in the Eulerian framework and evaluate the relationship between them.

4.1 *Spatial analysis*

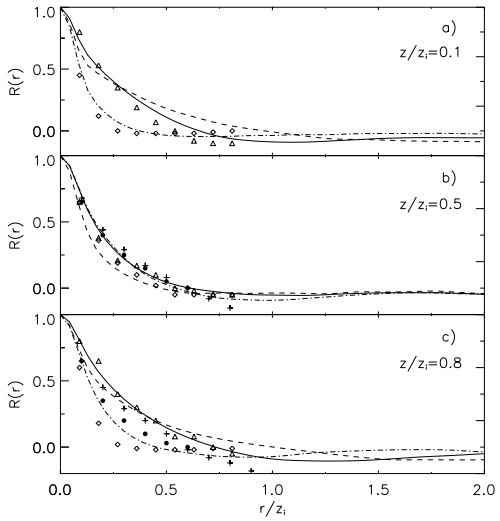

FIG. 1: Eulerian autocorrelation function $R^E(r)$ calculated at different heights as a function of the normalized space lag r/z_i. Continuous line: u-component, dashed line: v-component, dashed-dotted line: w-component. The following numerical and experimental data are also shown: diamonds and triangles, Mason (1989); circles and +, Deardorff and Willis (1985).

Fig. 1 shows the autocorrelation function for the three wind components calculated at three different heights ($z/z_i = 0.1$, $z/z_i = 0.5$, $z/z_i = 0.8$). The results show that while in the middle of the boundary layer the autocorrelation function for w does not differ significantly from the autocorrelation functions for u and v, in

the surface layer and in the upper part of the CBL the autocorrelation function for the vertical velocity decays more rapidly than for the horizontal components. Our results agree with previous numerical studies (Mason, 1989) and laboratory experiments (Deardorff and Willlis, 1985).
The length scales λ^E calculated as integral of the autorrelation (not shown) remain approximately constant with height between $z/z_i = 0.2$ and $z/z_i = 0.7$. In the region below $z/z_i < 0.2$ and in the entrainment zone, the length scales differ significantly from their mean value in the bulk of the CBL. In particular the vertical length scale decreases with height whereas the horizontal ones increase. This is a direct consequence of the non-homogeneity of the flow in the CBL, especially near to the ground (surface layer) and in the entrainment zone where the vertical motion is converted into horizontal (Moeng and Sullivan, 1994, Dosio et al, 2003).

4.2 *Temporal analysis*

Time series for the three velocity components were collected at 1024 points uniformly distributed in the horizontal domain for each vertical level. The autocorrelations for the three wind components have similar values to the ones calculated through spatial analysis. Our results agree with the data by Hanna (1981) who measured an averaged value of the Eulerian time scales of 50 s for all the wind components.

4.3 *Validation of Taylor's hypothesis of frozen turbulence in atmospheric flows*

As mentioned earlier, field experiments usually measure variables that evolve with time. As a result, the statistics are dependent on time. Laboratory experiments and numerical simulations, on the other hand, calculate statistics as function of space. The two frameworks are related by Taylor's hypothesis of frozen turbulence. Following Pasquill (1974), Taylor's hypothesis is applied to autocorrelations as follows:

$$R(t) = R(x) \qquad if \quad x = Ut \tag{9}$$

this in turn leads to the relationship between Eulerian length and time scales:

$$UT^E = \lambda^E \tag{10}$$

To our knowledge, this is the first time that length and time scales are calculated within the same experiment, allowing a direct validation of relation (10). The vertical profile of the ratio $\frac{1}{U}\frac{\lambda^E}{T^E}$ is close to one for all the wind components, which shows that Taylor's hypothesis (Eq. 9) holds in the simulated CBL.

5. LAGRANGIAN STATISTICS

Lagrangian statistics were calculated by following, both in space and time, the particles released at different positions in the simulated CBL. In Fig. 2 an example of particle trajectory (i.e. vertical position as function of the non dimensional time $t_* = (z_i/w_*)t$) is shown. The particle is released in the middle of the boundary layer ($z/z_i = 0.5$) and is rapidly caught by the thermals which transported it in a wave-like motion between the boundaries of the CBL. This motion, typical for strongly convective BL has a great influence on the shape of the Lagrangian autocorrelation, as it will be discussed.
In the same picture, the mean plume height (plume centerline) of particles released at three different heights ($z/z_i = 0.2, 0.5, 0.85$ respectively) is also shown. The vertical motion at short times after the release is largely dependent on the release height. As shown, particles released at $z/z_i = 0.2$ are caught by thermal and rise very quickly whereas particles released at $z/z_i = 0.8$ descend more slowly and remain in the upper part of the CBL for a long time. The difference in the particle motions at short times is related to the different vertical structure of the turbulent field in the CBL as explained by Moeng and Sullivan (1994).
At longer times ($t_* > 1$), all particles are (on average) in the middle of the CBL and therefore they have a similar behavior, moving in a periodic motion between the boundaries of the CBL.

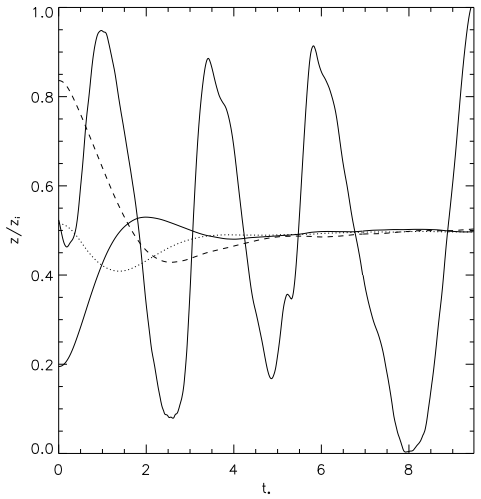

FIG. 2: Mean plume height (plume centerline) of particles released at three different heights ($z/z_i = 0.2, 0.5, 0.85$ respectively) and example of trajectory (vertical position as function of time) of a particle released at $z/z_{=}0.5$.

Lagrangian autocorrelations as a function of the dimensionless time t_* are shown in Fig. 3. They are presented as average over particles released at three different heights: particles released below $z/z_i = 0.25$, particles released between $z/z_i = 0.235$ and $zs/z_i = 0.75$ and particles released above 0.75.
There is a noticeable difference between the autocorrelation for the horizontal (v) and the vertical (w) wind component. The horizontal autocorrelation (Fig. 3a) closely follows an exponential decay (i.e. at $z/z_i = 0.5$ $R(\tau) = \exp(-\tau/200)$), characteristic of a Markov process. The shape of the autocorrelation is independent

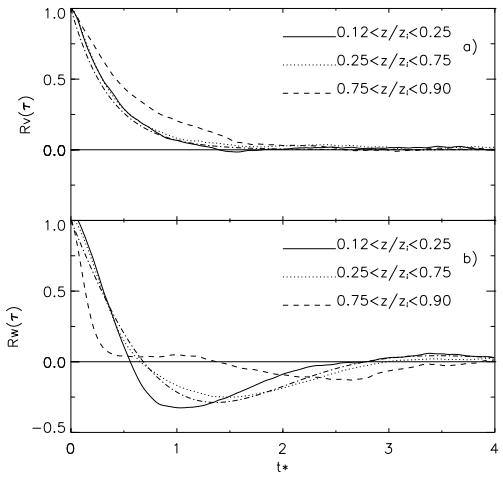

FIG. 3: a) Lagrangian autocorrelation for the horizontal (v) motion for particles released at different heights. The function $R(\tau) = \exp(-\tau/200)$ is also shown (dashed-dotted line). b) Lagrangian autocorrelation for the vertical (w) motion for particles released at different heights. Equation (11) is also shown (dashed-dotted line).

of the height of the release, but it is clear that the integral of the autocorrelation for particle released above $z/z_i = 0.75$ is slightly larger than the one for particles released in the middle of the CBL.

The vertical autocorrelation departs from an exponential function. The shapes of the autocorrelation of particles released below $z/z_i = 0.25$ or between $z/z_i = 0.25$ and $z/z_i = 0.75$ are quite similar and peculiar. Both have a strong minimum (respectively at t*=1 and 1.4) and they reach constant value close to zero at larger times. This particular shape of the autocorrelation is found for periodic (or wave-like) motions, as explained by Csanady (1973). In the CBL, the particles' vertical motion is limited by the bottom and the top boundaries and the particles move periodically within the CBL, as shown in Fig. 2. This autocorrelation is analytically reproduced by combining a stochastic motion (characterized by an exponential autocorrelation) and a wave-like motion (characterized by a sinusoidal autocorrelation). The resulting autocorrelation has a shape similar to the analytical function (Csanady, 1973):

$$R^L(\tau) = e^{-m\tau}\left(\cos(n\tau) - \frac{m}{n}\cos(n\tau)\right) \qquad (11)$$

As Fig. 3b shows, the function (11) with $m = 0.9$ and $n = 1.5$ fits accurately the LES results for the release at $z/z_i = 0.5$.

As said before, experimental measurements of Lagrangian statistics in the CBL are extremely rare. In his study, Hanna (1981) calculates the integral time arbitrarily assuming that T_L corresponds to the time lag at which $R(\tau)$ first drops to 0.37, therefore implicitly assuming an exponential shape for $R(\tau)$. However, he pointed out that the autocorrelation curves do not approach zero at the largest time lags available. This may implicate that his dataset (30' record) was too short to show the negative behavior of the autocorrelation function at large times.

In their study of synoptic scale Lagrangian autocorrelation function, Dauod et al (2002) analyzed a large database of modelled 10-day atmospheric trajectories and they show indeed an autocorrelation function whose shape is similar to that in our study (although in their case is the horizontal velocity autocorrelation). They also relate this shape to wave-like motion of the particle in the atmosphere.

Numerical investigations of Lagrangian statistics in turbulent flow are reported by Wang et al (1995) and Young and Pope (1989). The latter performed a DNS simulation of isotropic turbulence at relatively low Reynolds number (< 100) therefore their study s not directly comparable with atmospheric turbulence. Wang et al (1995) performed a LES simulation of a turbulent channel flow at Reynolds number of 21900, which can be regarded as an idealization of a neutral atmospheric boundary layer. In our opinion, particles released in a neutral BL have a different behavior compared to a pure-convective CBL. As shown by Dosio et al (2003) a tracer released in a near neutral BL is transported horizontally rather than vertically; the vertical dispersion is reduced whereas the horizontal dispersion is enhanced. Therefore, the vertical wave-like motion, which leads to the negative-shaped autocorrelation, is largely reduced in a neutral BL.

In fact, as Fig. 3b) shows, the shape of the autocorrelation for particles released above $z/z_i = 0.75$ (where structure of the thermals is different than in the bulk of the CBL) is much more close to an exponential shape, especially at short time. At longer time, when the particles are in the middle of the CBL the autocorrelation shows the negative minimum (but smaller than the other cases) and finally it reaches zero.

From the autocorrelation function the following function is calculated:

$$T_j^L(t) = \int_0^t R_j^L(\tau)d\tau \qquad (12)$$

By definition (6) the Lagrangian time T_j^L is therefore the limit for large times of $T_j^L(t)$.

Figure 4 shows the function $T_j^L(t)$ for the horizontal and vertical motion of particles released at different heights. For the horizontal motion, $T_v^L(t)$ grows constantly until it reaches a (fairly) constant asymptotic value. This asymptote represents the Lagrangian time (6) and it has a value $T_v^L = 250s$ for particles released below $z/z_i = 0.75$. The Lagrangian time for particles released above $z/z_i = 0.75$ has a larger value ($T_v^L = 320s$), as explained previously.

For the vertical motion, the curve $T_w^L(t)$ follows closely the one for the horizontal motion for short times before reaching a maximum and finally dropping to zero. The value and the position of the maximum depend on the release height, being $T_w^L = 175s$ for particles released below $z/z_i = 0.75$ and $T_w^L = 125s$ for particles released above $z/z_i = 0.75$.

It is therefore clear that in the atmospheric CBL the La-

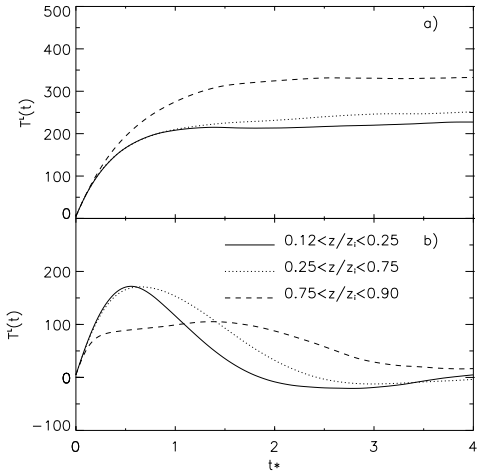

FIG. 4: Integral of the autocorrelation (12) for the horizontal (a) and vertical (b) wind components for particles released at different heights.

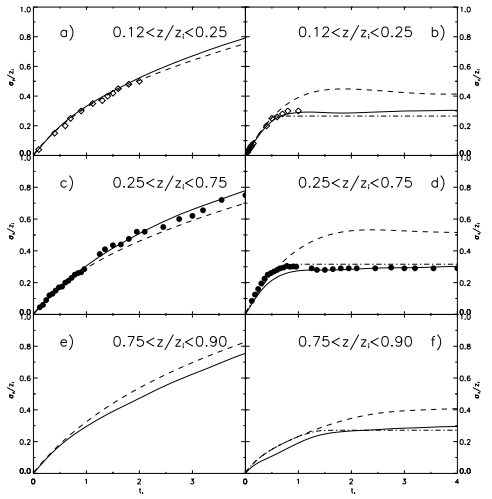

FIG. 5: a) Horizontal dispersion parameters calculated from the particle positions (1) (continuous line) and from Taylor's theory (2) (dashed line) for particles release below $z/z_i = 0.25$. The data (diamonds) from Lamb (1978) are also shown. b) Vertical dispersion parameters calculated from the particle positions (1) (continuous line) and from Taylor's theory (2) (dashed line) for particles release below $z/z_i = 0.25$. The dashed-dotted line represent expression (2) calculated using the function $T'_L(t)$. c) Same as a) for particles released between $z/z_i = 0.25$ and $z/z_i = 0.75$. The data (circles) from Willis and Deardorff (1981) are also shown. d) Same as b) for particles released between $z/z_i = 0.25$ and $z/z_i = 0.75$. d) Same as a) for particles released above $z/z_i = 0.75$. f) Same as b) for particles released above $z/z_i = 0.75$.

grangian properties at short times ($t < t_*$) depend on the release height. Moreover, a peculiar difference exists at large times between vertical and horizontal direction, due to the constrain imposed by the lower and upper boundaries to the vertical motion. These effects have a large influence on the autocorrelation shape and the value of the Lagrangian time, as shown. This difference between horizontal and vertical motion has also a great effect on the particle displacement (dispersion), as it will be discussed in the next Section.

6. ANALYSIS OF TAYLOR'S DISPERSION RELATIONSHIP

In this section the relationship between the flow characteristics and the particles' displacement (dispersion) is analyzed. The displacement of the particle ensemble $\overline{x_j'^2}(t)$ (1) is related to the Lagrangian autocorrelation through Taylor's diffusion theory (2). By using the LES results, the two functions (1) and (2) are calculated and compared in Fig. 5.

6.1 *Horizontal dispersion*

For the horizontal motion (Fig. 5a, 5c 5e) Taylor's theory is satisfactorily fulfilled. The displacement $\overline{y'^2}(t)$ of particles released below $z/z_i = 0.25$ and between $z/z_i = 0.25$ and $z/z_i = 0.75$ agrees with previous studies and laboratory measurements respectively. (Lamb, 1978, Willis and Deardorff, 1981). Equation (2) follows closely the displacement curve, and it shows the expected limits at short and long times, respectively $\sigma_v t$ and $2\sigma_v (T_v^L t)^{1/2}$. This result is related to the exponential shape of the autocorrelation (Fig. 3), leading to a constant limit at long times for the value of the Lagrangian integral time (Fig. 4).

6.2 *Vertical dispersion*

The comparison between the particle displacement $\overline{z'^2}(t)$ and equation (2) for the vertical motion is less satisfactory and requires a more detailed analysis and discussion. The results strongly depend on the particle release height, since they are a function of the autocorrelation and the integral scale.

6.2.1 *Particles released below* $z/z_i = 0.75$

The vertical displacement (1) calculated from the particle trajectories agrees with previous experiments and reaches a constant limit of $\overline{z'^2}(t) \sim 0.3$, characteristic of an ensemble of particles uniformly mixed within the CBL (fig. 5b and 5d). Equation (2), on the other hand, agrees with the displacement and previous experiments only at short times ($t_* < 0.7$). This time is of the same order of magnitude as the turnover time and corresponds to the period when the particles, just after being released, are still unaffected by the CBL boundaries. In other words, the particles are in a regime of "free motion". As Fig. 5b shows, at longer times equation (2) reaches a constant limit of about 0.5. This limit is due to the peculiar shape of the autocorrelation for vertical motion for $t_* > 2$,

which leads to $T_w^L = \lim_{t\to\infty} T_w^L(t) \simeq 0$ (see Fig. 4b). As a result, equation (2) becomes:

$$\overline{x_j^{'2}}(t) \sim \int_0^t \int_0^{t'} R_w^L(\tau) d\tau dt' = \int_0^t T_w^L(t') dt' = const \tag{13}$$

As mentioned earlier, Taylor's diffusion theory was developed for homogeneous turbulence, whereas the CBL is characterized by non homogeneous turbulence and vertically bounded motion. Therefore we consider more appropriate to distinguish between free and bounded motion, as discussed later.

6.2.2 *Particles released above* $z/z_i = 0.7$

Particles released in the upper layers are affected by the different structure of the turbulence in the upper layer of the CBL. The vertical motion at short times is reduced (see Fig. 2) and the vertical displacement diminished. At longer times ($t_* > 1.5$) the particles are well mixed within the entire CBL and the displacement (1) reaches the constant limit of about 0.3 as explained earlier. However, also in this case, equation (2) overestimates this limit at longer times.

6.2.3 *Distinction between free and bounded motion*

A more adequate interpretation of the LES results with respect to expression (2) is obtained if the two regimes (free motion and bounded motion) are considered separately, in other words, when a distinction is made between shorter and longer times after the release. As previously shown, the period of time in which the particles are in a regime of free motion (before being affected by the CBL boundaries) is of the same order of magnitude as the turnover time. Let t_0 is the time at which the function $T_w^L(t)$ reaches its maximum value. A new characteristic time scale is defined as:

$$T_L^{'}(t) = T_w^L(t) \qquad t \le t_0 \tag{14}$$

$$T_L^{'}(t) = 0 \qquad t > t_0 \tag{15}$$

This function is consistent with the two limits (for shorter and longer times) that the function $T_w^L(t)$ must fulfill.
If we now recalculate (2) using the new function $T_L^{'}(t)$, the results agree more satisfactorily with the experiments and the particle displacement $\overline{z'^2}$, as shown in Fig. 5b, 5d and 5f.

7. RELATION BETWEEN EULERIAN AND LAGRANGIAN FRAMEWORKS

7.1 *Integral Lagrangian time scale*

Figures 6a and 6c show the vertical profiles of time scales T_j^L. Both the horizontal and the vertical Lagrangian time scales are almost constant with height for $z/z_i < 0.75$. The vertically averaged values below $z/z_i < 0.75$ are $T_v^L = 220\ s$ and $T_w^L = 180\ s$ respectively. Our results are in agreement with the measurements by Phillips and Panofsky (1982) ($T_v^L \sim 190\ s$). Other previous experimental studies show a large uncertainty in the value of the Lagrangian time. For instance, atmospheric measurements range from $70 - 80s$ (Hanna, 1981) to $10^4 s$ (Gifford, 1982). The numerical studies by Wang et al. (1995) and by Uliasz and Sorbjan (1999) do not provide a direct value of the calculated integral time scale. As pointed out by Hanna (1981), atmospheric measurements are influenced by the complexity of the experimental setup and the short sampling time. Moreover, the results depend on different meteorological conditions during the measurement campaign. The LES results, on the contrary, are obtained from a more controlled experiment and from a longer time series of data.
The value of the Lagrangian time scale is commonly pa-

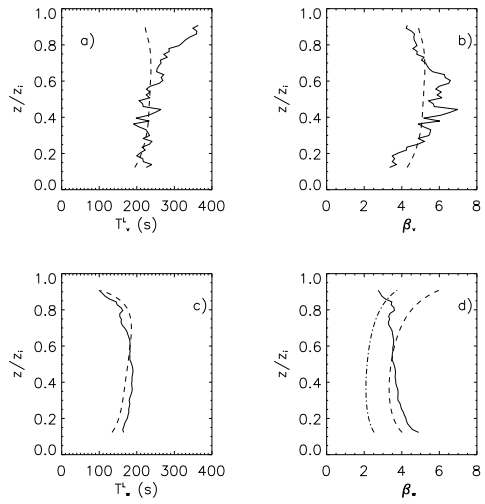

FIG. 6: a) Vertical profiles of horizontal Lagrangian time scale as calculated by LES (continuous line) and parameterized according to (16) (dashed line). b) Ratio between the horizontal Lagrangian and Eulerian time scales as calculated by LES (continuous line) and parameterized according to (18) (dashed line). c) Same as a) for the vertical wind component. The dashed line represents the parameterization (17). d) Same as b) for the vertical wind component. Expression (18) for $C = 0.4$ is shown as dashed-dotted line.

rameterized as a function of CBL Eulerian characteristics (Angell, 1964). According to Degrazia et al. (1998):

$$T_v^L = 0.17 \frac{z_i}{\sigma_v} \tag{16}$$

$$T_w^L = 0.2 \frac{z_i}{\sigma_w} \left[1 - \exp(-8z/z_i) - 0.0003 \exp(8.5 z/z_i)\right] \tag{17}$$

As shown by Degrazia et al. (1998), equations (16) and (17) agree with the atmospheric measurements by Hanna (1981) in the middle of the CBL. In Fig. 6a and 6c expressions (16) and (17) are compared with the LES results.

Both parameterizations are able to reproduce the LES results correctly for heights below $z/z_i = 0.75$.
Above $z/z_i = 0.75$ the LES results show an increase of T_v^L with height (Fig. 6a).

7.2 *Value of the ratio* β_j

Figures 6b and 6d show the ratio β_j of the Lagrangian to Eulerian timescales for the horizontal and vertical wind component. For the horizontal wind component, β_v varies between 4 and 6, with a vertically averaged value of $\beta_v = 5$. The irregular vertical profile of β_v is due to fluctuations in the autocorrelation function (Fig. 3a). For the vertical wind component, the values of β_w calculated by the LES has a vertically averaged value of 4. Values in literature range form 1.8 (Hanna, 1981) to 4 Aangell (1964).
The value of β_j is usually related to the intensity of turbulence $i = \sigma_j/U$ by (**??**). In Fig. 6b the following parameterization proposed by Hanna (1981) is also shown:

$$\beta_j = C\frac{U}{\sigma_j} = 0.7\frac{U}{\sigma_j} \tag{18}$$

As it can be seen, despite the fluctuations, the parameterization is in satisfactory agreement with the LES results.
As shown in Fig. 6d the parameterization (18) for the vertical component agrees with the LES results only for $z/z_i < 0.7$. Other values of the constant C range in the literature from 0.35 to 0.8 as reported by Pasquill (1974). Theoretical analysis by Wandel and Kofoed-Hansen (1962) leads to $C = 0.44$ whereas the numerical simulation by Wang et al. (1995) gives a value of $C = 0.6$. To illustrate the dependence of the parameterization on the value of the constant C, expression (18) is shown in Fig. 6d for two values of the constant, respectively $C = 0.4$ and $C = 0.7$. As stated by Hanna (1981) the value $C = 0.7$ gives the best fit for the overall dataset, whereas the value $C = 0.4$ fits better the experimental data for high wind speed and it is in better agreement with the LES results in the upper layers of the CBL.

8. CONCLUSIONS

Eulerian and Lagrangian statistics were calculated by means of a LES. A large numerical domain and a long integration time were used in order to obtain reliable statistics both in space and in time.
Three main research issues were studied. First, Eulerian statistics were calculated by means of spatial and temporal analysis. The two frameworks are related by Taylor's hypothesis of frozen turbulence. Characteristic length and temporal scales were derived through the analysis of the autocorrelation allowing a direct validation of Taylor's hypothesis, which results satisfied in the simulated CBL.
Second, the relationship between flow properties (autocorrelations) and dispersion characteristics (particles' displacements) was discussed through Taylor's analysis of turbulent dispersion. The influence of the asymmetry of the CBL flow on dispersion was discussed, with the focus being on the difference between horizontal and vertical motion, because the latter is influenced by the presence of the surface and the strong inversion at the top of the CBL. Results showed that for the horizontal velocity the autocorrelation had an exponential shape, characteristic of a stochastic motion. As a result, horizontal dispersion was satisfactorily described by Taylor's theory.
On the contrary, the autocorrelation function for the vertical velocity had a more complicate shape, due to the wave-like motion of the particles confined between the CBL boundaries. As a result, the value of the integral scale was zero. Taylor's analysis predicted correctly the particles' displacement at short times, but overestimated the asymptotic limit at longer times.
The use of a different method to calculate the Lagrangian integral time (14), allowed us to distinguish better between free and bounded motion, and a better agreement between Taylor's relationship and particles' vertical displacement was found.
Finally, the relationship between Lagrangian and Eulerian framework was investigated through the calculation of the Lagrangian integral scales and the ratio β. Vertical profile of T_j^L showed that the integral scales remain constant at heights $z/z_i = 0.7$. The difference in the turbulence characteristics near to the inversion, influenced the particles' motion, which is transformed from vertical into horizontal. This affected the values of the integral scales in the upper layers of the CBL, where the horizontal time scale increased, whereas the vertical was reduced. Currently used parameterizations for the ratio β, derived either in previous field atmospheric experiments or through theoretical analysis were compared with the LES results, showing a satisfactory agreement.

Acknowledgements

Discussions and comments by Stefano Galmarini, Harm Jonker, Han van Dop, Arjan van Dijk and Jeffrey C. Weil have been very useful and deeply appreciated. A.Dosio is funded within the Centre of Expertise Emissions and Assessment - a cooperation between TNO and Wageningen University. All the numerical simulations have been performed on the TERAS supercomputer of the National Computing Center SARA (project number 2003/00302)

References

Angell, J. K., 1964: Measurements of Lagrangian and Eulerian of turbulence at a height of 2500 ft, *Quart. J. Roy. Meteor. Soc.*, **90**, 57–71.

Csanady, G. T., 1973: *Turbulent diffusion in the environment*. D. Reidel Publishing company, 248 pp.

Daoud, W. Z., J. W. D. Kahl, and J. K. Ghorai, 2002: On the synoptic-scale Lagrangian autocorrelation function, *J. Appl. Meteorol.*, **42**, 318–324.

Deardorff, J. W., and G. E. Willis, 1985: Further results froma a laboratory model of the convective planetary boundary layer, *Bound.-Layer Meteo.*, **32**, 205–236.

Degrazia, G., D. Anfossi, H. F. D. C. Velho, and E. Ferrero, 1998: A Lagrangian decorrelation time scale

in the convective boundary layer, *Bound.-Layer Meteo.*, **86**, 525–534, 1998.

Dosio, A., J. Vilà-Guerau de Arellano, A. A. M. Holtslag, and P. J. H. Builtjes, 2003: Dispersion of a passive tracer in buoyancy- and shear-driven boundary layers, *J. Appl. Meteorol.*, **42**, 1116–1130.

Gifford, F. A., 1982: Horizontal diffusion in the atmosphere: a Lagrangian-dynamical theory, *Atmos. Environ.*, **16**, 505–512.

Gopalakrishnan, S. G., and R. Avissar, 2000: An LES study of the impacts of land surface heterogeneity on dispersion in the convective boundary layer, *J. Atmos. Sci.*, **57**, 352–371.

Hanna, S. R., 1981: Lagrangian and Eulerian timescale relations in the daytime boundary layer, *J. Appl. Meteorol.*, **20**, 242–249.

Holtslag, A. A. M., and F. T. M. Nieuwstadt, 1986: Scaling the atmospheric boundary layer, *Bound.-Layer Meteo.*, **36**, 201–209.

Lamb, R. G., 1978: A numerical simulation of dispersion from an elevated point source in the convective planetary boundary layer, *Atmos. Environ.*, **12**, 1297–1304.

Mason, P. J., 1989: Large-eddy simulation of the convective boundary layer, *J. Atmos. Sci.*, **46**, 1492–1516.

Moeng, C.-H., and P. P. Sullivan, 1994: A comparison of shear- and buoyancy-driven planetary boundary layer flows, *J. Atmos. Sci.*, **7**, 999–1022.

Pasquill, F., 1974: *Atmospheric diffusion*. Ellis Horwood Limited, 429 pp.

Phillips, P., and H. A. Panofsky, 1982: A re-examination of lateral dispersion from continuous sources, *Atmos. Environ.*, **16**, 1851–1859.

Sato, Y., and K. Yamamoto, 1987: Lagrangian measurements of fluid-particle motion in an isotropic turbulent field, *J. Fluid Mech.*, **175**, 183–199. 200, 511–562.

Siebesma, A. P., and J. W. M. Cuijpers, 1995: Evaluation of parametric assumptions for shallow cumulus convection, *J. Atmos. Sci.*, **52**, 650–666.

Taylor, G. I., 1921: Diffusion by continuous movements, *Proc. Roy. Soc. Ser.*, **A20**, 196–211.

Uliasz, M., and Z. Sorbjan, 1999: Lagrangian statistics in atmospheric boundary layer derived from LES, *13th Symposium on Boundary Layers and Turbulence*, American Meteorological Society, p. P2A.6.

Vreugdenhil, C. B., and B. Koren (eds.), 1993: Numerical methods for advection-diffusion problems, *Numerical fluid mechanics*, Vieweg.

Wandel, C. F., and O. Kofoed-Hansen, 1962: On the Eulerian-Lagrangian transform in the statistical theory of turbulence, *J. Geophys. Res.*, **76**, 3089–3093.

Wang, Q., K. D. Squires, and X. Wu, 1995: Lagrangian statistics in turbulent channel flow, *Atmos. Environ.*, **29**, 2417–2427.

Weil, J. C., P. Sullivan, C. H. Moeng, 2004: On the use of Large-Eddy Simulations in Lagrangian particle dispersion models, *J. Atmos. Sci.*,accepted for publication.

Willis, G. E., and J. W. Deardorff, 1981: A laboratory study of dispersion from a source in the middle of the convectively mixed layer, *Atmos. Environ.*, **15**, 109–117.

Yeung, P. K., and S. B. Pope, 1989: Lagrangian statistics from direct numerical simulations of isotropic turbulence, *J. Fluid Mech.*, **207**, 531–586.